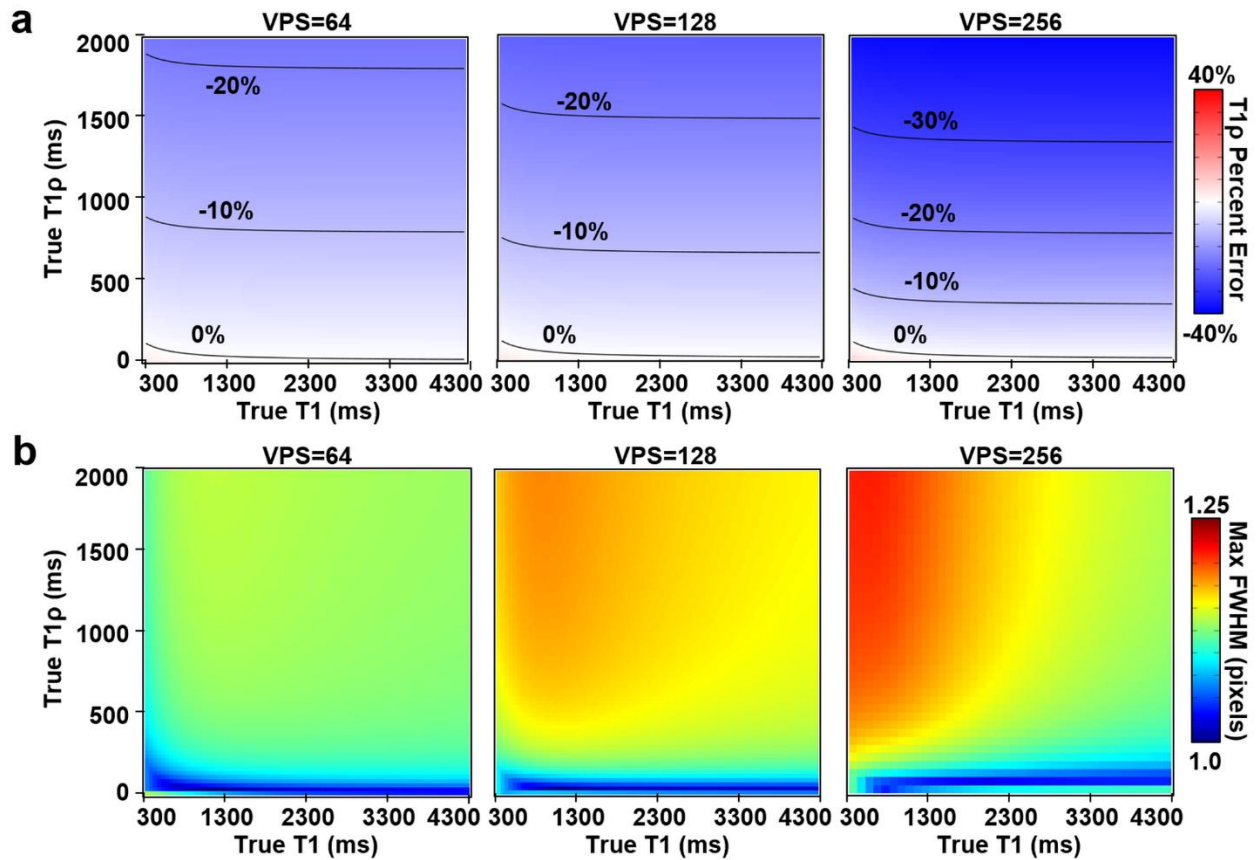
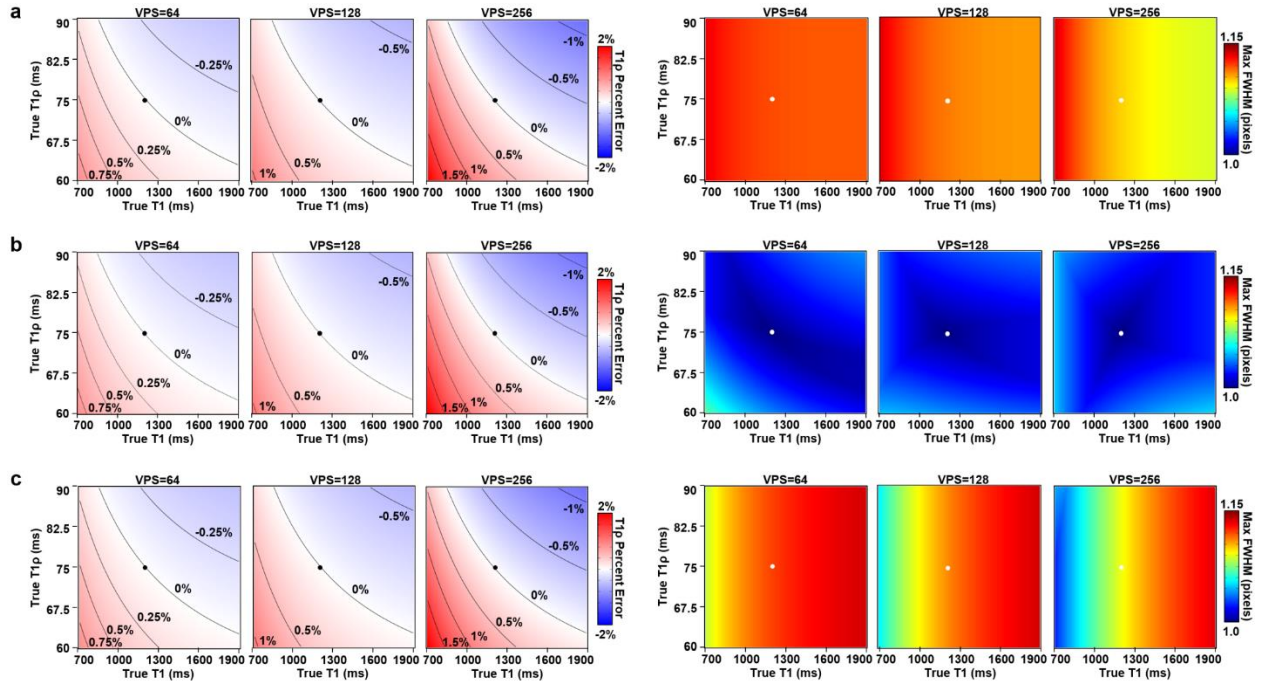


SUPPORTING INFORMATION

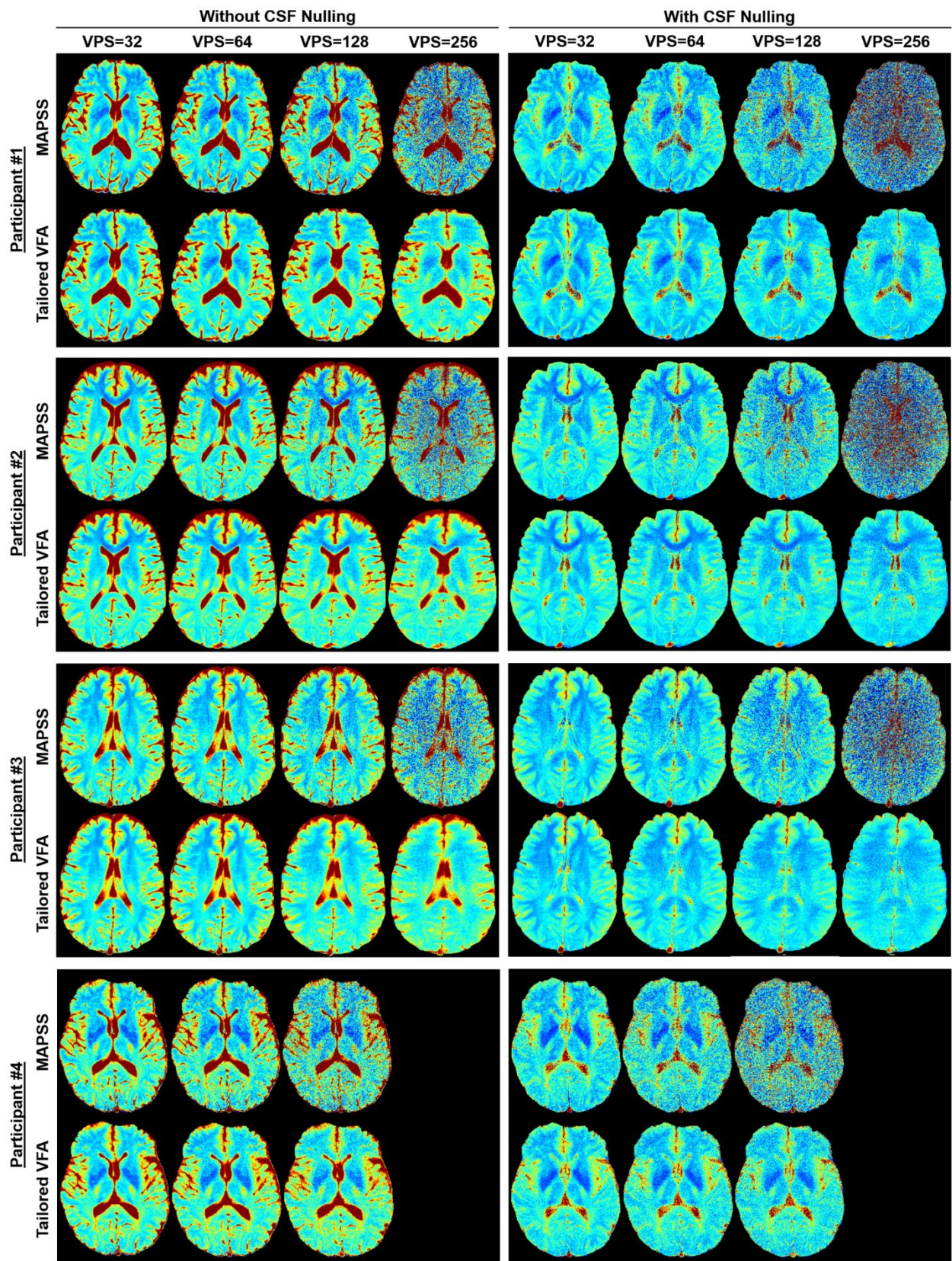
Supporting Information Figure S1: Simulated (a) T1 ρ percent error and (b) spatial blurring for a extended range of true T1 ρ and T1 values up to those expected for CSF. Plots are shown in the same manner as Figure 4a-b. T1 ρ is not accurately quantified for fluid, with errors increasing to 20% or more. Voxels with CSF also have increased spatial blurring compared to voxels with just brain tissue. CSF nulling may help reduce these confounding signals.



Supporting Information Figure S2: Simulated T1 ρ percent error and spatial blurring over the range of typical brain tissue T1 ρ and T1 values for three different flip angle scaling factors due to transmit B1-field inhomogeneity: **(a)** 0.8; **(b)** 1.0; and **(c)** 1.2. The plots in **(b)** are the same as those in Figure 4 (no B1 inhomogeneity). The B1 inhomogeneity in **(a)** and **(c)** does not affect the T1 ρ percent error, but it does increase spatial blurring.

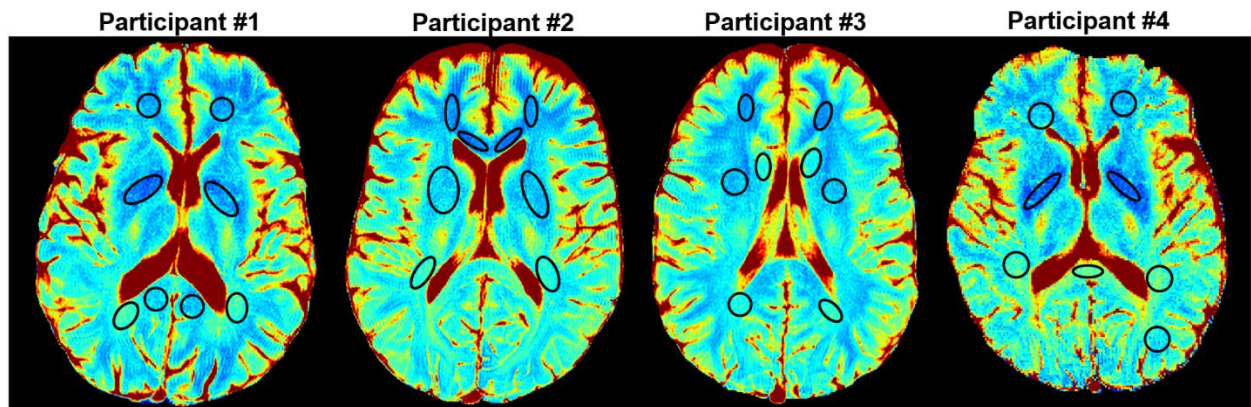


Supporting Information Figure S3: 2D T1 ρ maps for all four participants. The scan times were the same for a given VPS setting: 229, 125, 73, and 48 sec for VPS=32, 64, 128, and 256, respectively. The results are consistent across all four volunteers. The relative SNR efficiency of tailored VFA scheduling versus MAPSS increases with VPS while quantitatively the maps appear similar. However, there is also gradual loss of spatial fidelity for tailored VFA scheduling as VPS increases. Note that data at VPS=256 was not acquired for Participant #4.

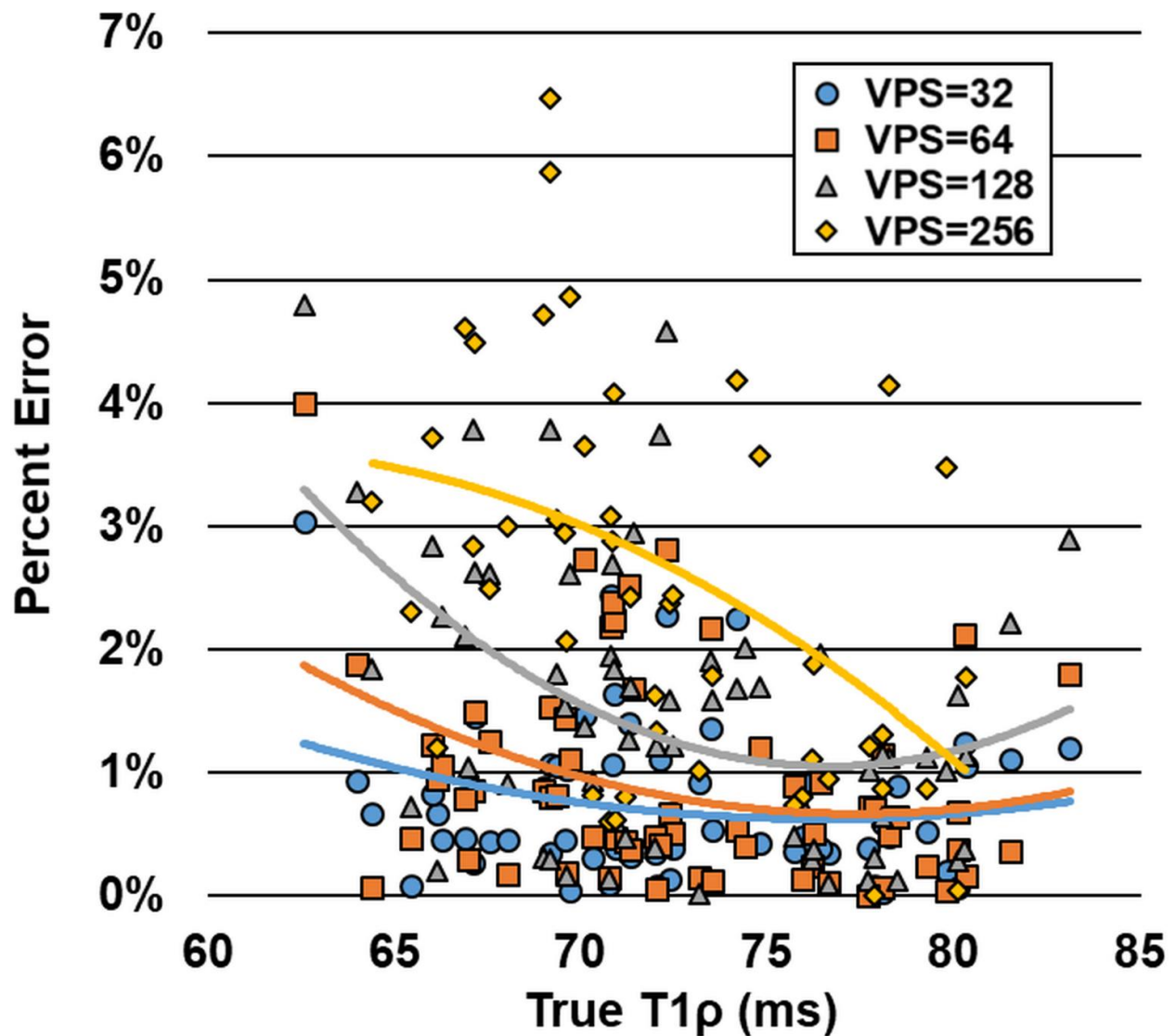


T1 ρ =50 ms 120 ms

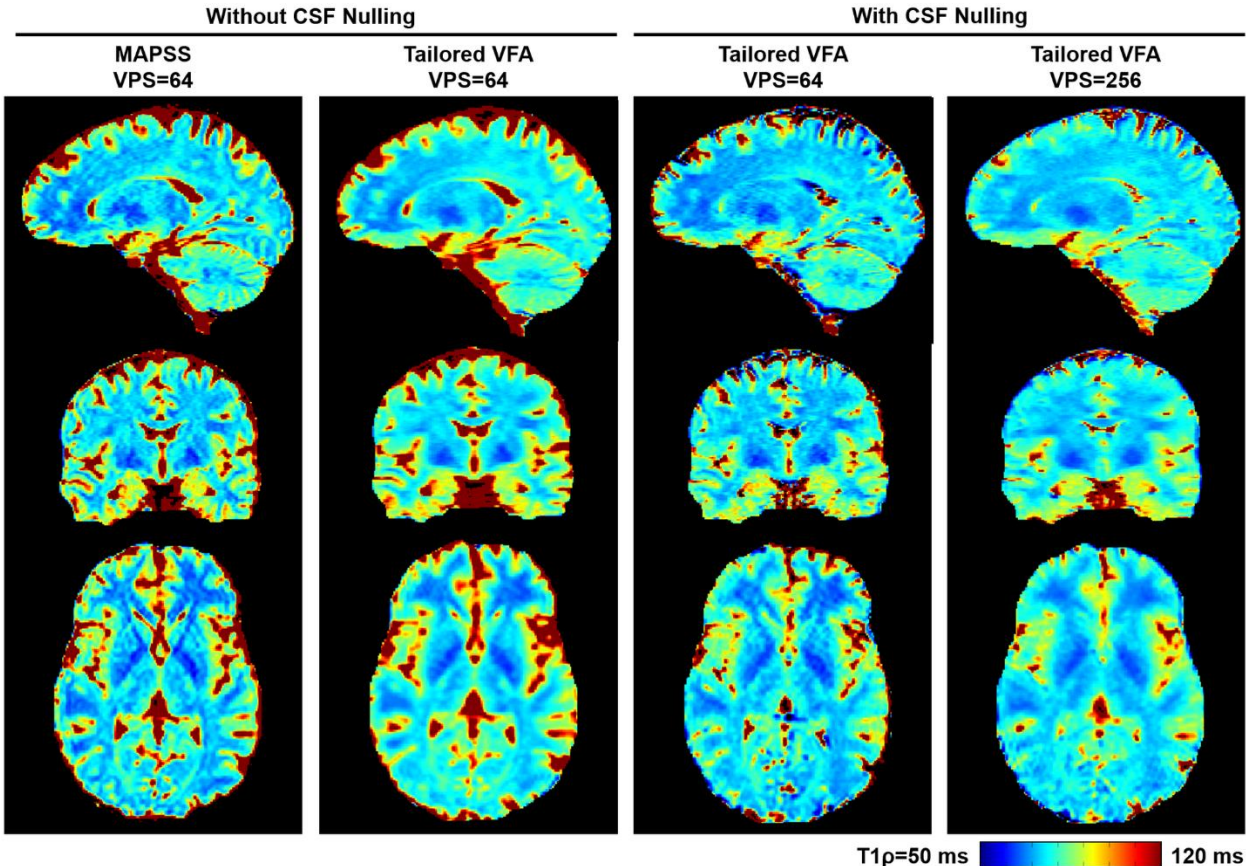
Supporting Information Figure S4: Locations of the eight ROIs used to calculate mean $T1\rho$ relaxation times for each participant's 2D $T1\rho$ maps.



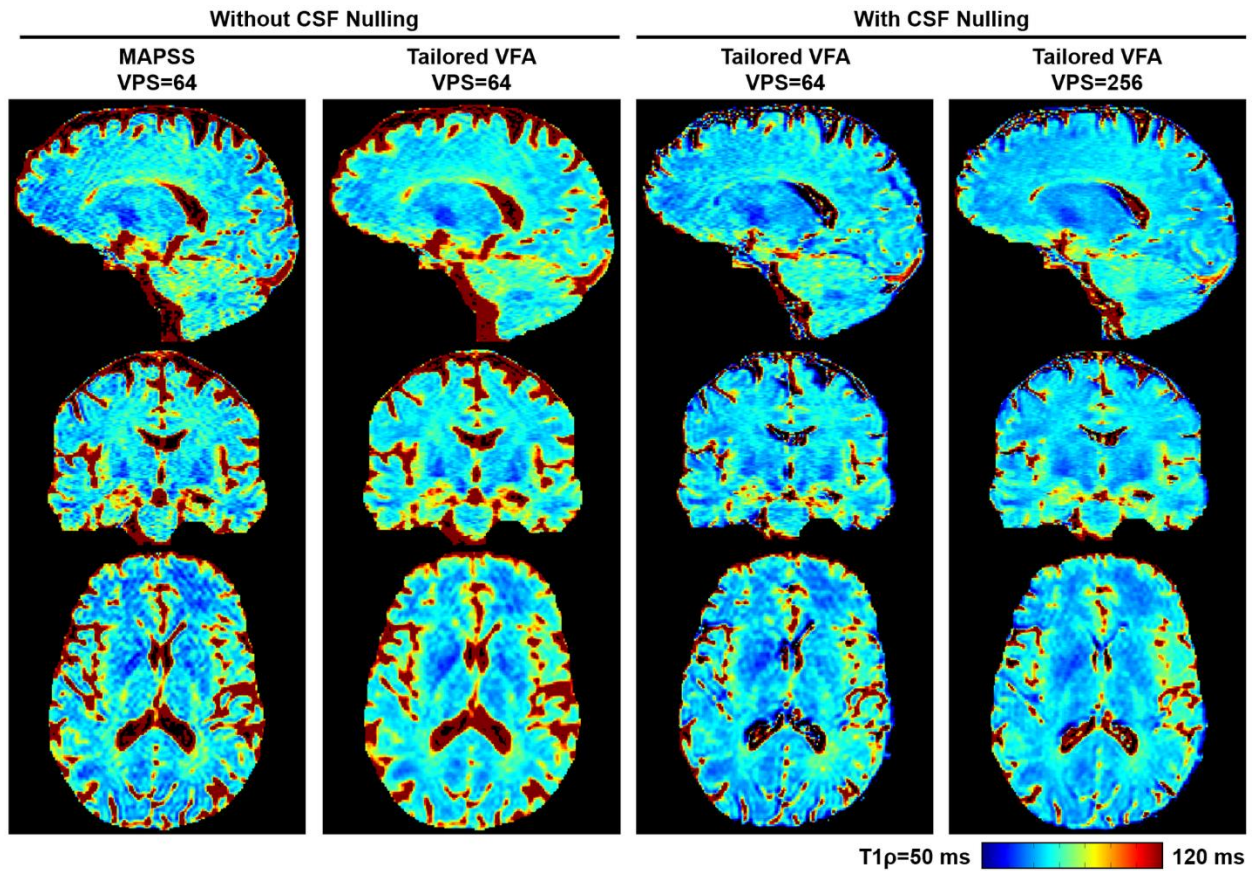
Supporting Information Figure S5: T1 ρ quantification error for tailored VFA scheduling versus true T1 ρ value (as measured by MAPSS at VPS=32) for all regions of interest (ROIs) for the 2D T1 ρ map data analyses (Supporting Information Figure S4). Data are included from T1 ρ maps acquired both with and without CSF nulling. Each point is a different ROI, and second-order polynomial trendlines are plotted for data at each VPS. For all VPS, errors are generally lowest near T1 ρ =75 ms (the assumed value for T1 ρ when generating the tailored VFA schedules) and slightly increase over the full range of measured T1 ρ values.



Supporting Information Figure S6: 3D T1 ρ maps for a second participant, shown in the same format as Figure 8.



Supporting Information Figure S7: 3D $T1\rho$ maps for a third participant, shown in the same format as Figure 8. This participant had consistent respiratory motion, which led to some motion artifacts in the $T1\rho$ maps.



Supporting Information Figure S8: ROI analysis of the relative SNR of the 3D T1 ρ datasets acquired with tailored VFA scheduling versus MAPSS. **(a)** Locations of the eight 2D ROIs used to calculate mean T1 ρ relaxation times for each participant's 3D T1 ρ maps. The ROIs were defined using the shown T1 ρ map 2D phase-encoding plane slices acquired with MAPSS. **(b)** Average relative SNR for tailored VFA scheduling (Datasets 2, 3, and 4) versus MAPSS (Dataset 1; see Table 2 and Figure 5 for dataset definitions) across the eight ROIs (error bars show the standard deviation). Each bar is a different participant. Average relative SNR across the participants was 1.5, 1.2, and 1.5 for Datasets 2, 3, and 4, respectively, which agrees well with the expected values from simulation (1.6, 1.1, and 1.6).

